Computers & Geosciences 159 (2022) 104981

Contents lists available at ScienceDirect

Computers and Geosciences

journal homepage: www.elsevier.com/locate/cageo

Grade estimation using a hybrid method of back-propagation artificial neural network and particle swarm optimization with integrated samples coordinate and local variability

Saeed Soltani-Mohammadi [a,*], Fatemeh Sadat Hoseinian [b], Maliheh Abbaszadeh [a], Mahdi Khodadadzadeh [c]

[a] *Department of Mining Engineering, University of Kashan, Kashan, Iran*
[b] *Department of Mining and Metallurgical Engineering, Amirkabir University of Technology, Tehran, 158754413, Iran*
[c] *Faculty of Geo-Information Science and Earth Observation (ITC), University of Twente, 7500, AE, Enschede, the Netherlands*

ARTICLE INFO

Keywords:
Grade estimation
Machine learning methods
Input space configuration
Parameter optimization

ABSTRACT

Grade estimation is a critical issue in mineral resource evaluation, being extensively investigated by data mining techniques. In this paper, a hybrid method composed of back-propagation artificial neural network (BPANN) and particle swarm optimization (PSO) algorithms is proposed to solve the grade estimation problem. The PSO algorithm is implemented to optimize the BPANN parameters by reducing the effects of a local minimum problem, which is one of the critical drawbacks of BPANN. The proposed BPANN-PSO algorithm is validated for Al_2O_3 grade estimation in one of Iran's largest Bauxite deposits. The performance of BPANN-PSO algorithm for grade estimation is compared with BPANN and ordinary kriging. The experimental results indicate that the BPANN-PSO model is more appropriate for estimating Al_2O_3 grade with a reasonable error.

1. Introduction

The grade block model is a key input to the production planning, scheduling, and financial analyses of mines (Sinclair and Blackwell 2002; Rendu 2014; Kaplan and Topal 2020). Since samples taken from deposits are limited in number, this task is usually subjected to estimation. Due to the very complex and, sometimes, not completely well-understood orebody deposition processes, grade estimation is quite a complicated problem (Kapageridis and Denby 1999). Most mining software programs offer traditional tools such as the nearest neighbor, inverse distance weighting, and geostatistical methods for estimating grades. For instance, Kriging is the most common and widely used geostatistical approach for grade estimation (Yamamoto 1999). Structural analysis (i.e., calculating the experimental variogram and fitting an appropriate model to it) is necessary to use geostatistical models. However, performing structural analysis is a challenging task, especially if the number of available samples is limited. The effective use of such traditional techniques requires assumptions, knowledge, skill, and long processing time (Wu and Zhou 1993; Kapageridis and Denby 1999). Therefore, the ongoing research is centered on the machine learning based methods for grade estimation. Artificial Neural Networks (ANNs) (Samanta et al. 2005; Chatterjee et al., 2006; Guo 2010; Li et al., 2010; Tahmasebi and Hezarkhani 2010, 2012; Mahmoudabadi et al., 2009; Singh et al., 2018), Adaptive Neuro-Fuzzy Inference System (ANFIS) (Tahmasebi and Hezarkhani 2010), random forest (Jafrasteh et al. 2016, 2018), Support Vector Machines (SVM) (Matias et al., 2004; Tenorio et al., 2015; Dutta et al., 2010) and combined kNN-ANN methods (Kaplan and Topal 2020) are the widely used algorithms. Among the others, ANNs are the most studied algorithms for the grade estimation. Several works have been published in the literature to investigate the effects of using different training algorithms (Samanta et al. 2005, 2006; Jafrasteh and Fathianpour 2017; Jafrasteh et al., 2018; Kaplan and Topal 2020), optimizing the weights of ANNs through genetic algorithm (Mahmoudabadi et al., 2009; Tahmasebi and Hezarkhani 2012), the configuration of the input space of ANNs (Kapageridis 2005), using wavelet neural network (Li et al., 2010) and neural-fuzzy systems (Tahmasebi and Hezarkhani 2010). Despite all these studies, no specific conclusion has yet been drawn regarding the preference of ANNs over traditional models. Although some researches show better results with ANNs (Chatterjee et al., 2006; Dutta et al., 2010; Badel et al., 2011;

* Corresponding author.
E-mail addresses: saeedsoltani@kashanu.ac.ir, saeedsoltani@kashanu.ac.ir (S. Soltani-Mohammadi).

https://doi.org/10.1016/j.cageo.2021.104981
Received 27 February 2021; Received in revised form 29 October 2021; Accepted 2 November 2021
Available online 9 November 2021
0098-3004/

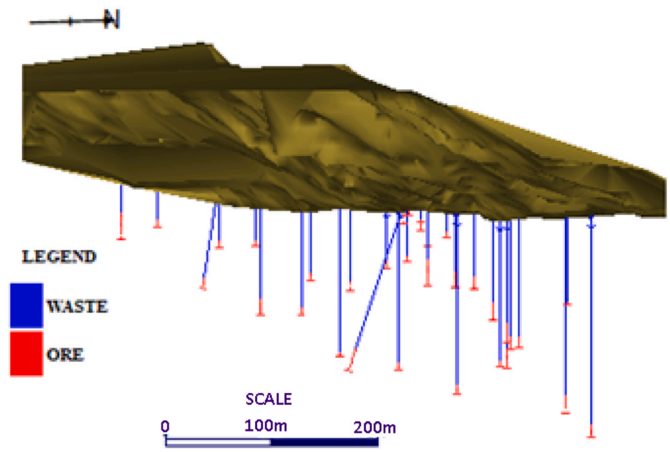

Fig. 1. Topography condition and drilled exploratory drill holes in Jajarm deposit (view direction: Azi 290, dip 5).

Jafrastehet al. 2018), others do not report any specific preference in comparison with the traditional geostatistical models (Samanta 2002; Samanta et al., 2005).

In ANN architecture, the weighted links and bias values - calculated based on the characteristics of input/output data - connect the network neurons (Hoseinian et al. 2017, 2018). Among the various types of ANN architectures, the back-propagation artificial neural network (BPANN) is the most widely used form of ANNs. It minimizes the error at each iteration (according to the gradient descent algorithm) and grants the best solution. The BPANN optimization begins by setting the vector of initial weights and stops according to the stopping criterion. BPANN has the universal advantages of self-learning, self-adaptive and nonlinear mapping ability (Changwei et al., 2019). Nevertheless, BPANN has various shortcomings, for instance, it can easily fall into a local minimum and have a slow convergence rate in the learning process (Hoseinian et al., 2019). To overcome local minima, the authors in (Qi et al., 2018) showed that the performance of ANN can be improved by using optimization of the initial weights and the threshold of the ANN applying the particle swarm optimization (PSO) and the genetic algorithms (Qi et al., 2018). In this paper, we adopt this idea and optimize the ANN weights and bias using the PSO method to promote its quality in grade estimation.

The input space configuration of machine learning-based methods defines how the estimated value is approached (Kapageridis 2005). Only two types of input space configuration are found in the literature. The most popular configuration is the samples' coordinate in the 2D or 3D space (Wu and Zhou 1993; Kapageridis and Denby 1999; Chatterjee et al., 2006; Samanta and Bandopadhyay 2009; Dutta et al., 2010; Tahmasebi and Hezarkhani 2010, 2012; Abbaszadehet al. 2016; Jafrasteh et al., 2018). This configuration considers grade as a function of samples' coordinates and defines the projection from the input coordinate space to the grade vectors during training (Kapageridis 2005). This input space configuration is successfully applied in the grade estimation of various types of deposits. The second strategy considers the local variability around each sample. The estimation problem becomes finding the relation between surrounding samples (their grades and distances to estimation point) and grade of estimation point. This strategy could consider the local variability in modeling (Kapageridis and Denby 1998). In this research, these configurations are combined to consider both the coordinate of the estimation point and local variability as the input space configuration. Finally, the performance of models trained based on the various configurations is compared.

2. Data sets

The layered Jajarm bauxite ore deposit, located 18 km north of Jajarm in North Khorasan, has more than 8 km in length and 20 m in depth, being the largest bauxite deposit in Iran (Esmaeily et al., 2010). The shape of ore suggests that it is Karst-Mediterranean style and bauxite reserves are layered-lens shapes with east-west direction. Due to various faulting in the area, the ore is divided into several blocks. The "Zu2" block is one of them. The total number of 72 exploratory boreholes has been drilled in this block to identify the geological, lithological, structural and chemical characteristics of orebody. These drill holes have been designed based on the relative distance to outcrop and topography conditions. The drilling has been carried out until the footwall of the bauxite layer has been intersected. Consequently, the depth of these drillholes has been increased with the distance from the bauxite outcrop. The deeper is a drill hole, the higher is the cost of drilling. Therefore, in the area distant from the outcrop, the number of drillholes has been decreased (i.e., spacing in the pattern has been increased). The drilling pattern and topography of the site are shown in Fig. 1. Nearby the bauxite outcrop, the average drillhole spacing ranges between 15 and 30 m. In the deeper or less explored areas, the average drillhole spacing ranges between 70 and 100 m. Constant profiles of Kaolinite clay, hard

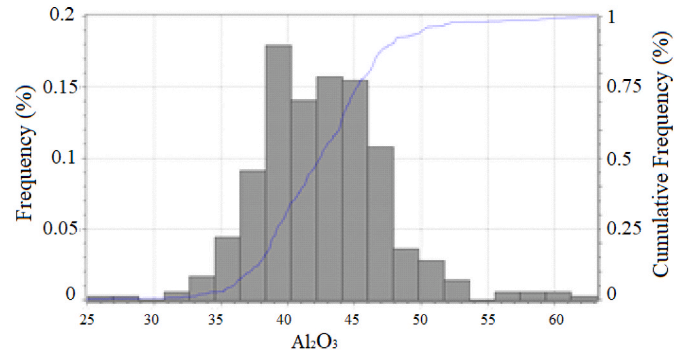

Fig. 2. Histogram of Al_2O_3.

Table 1
Statistical parameters of Al_2O_3.

Median	41.62
Mean	42.53
Min	25
Max	63.15
Standard Deviation	4.73
Variance	22.46
CV	0.11
Skewness	0.62
Kurtosis	2.49

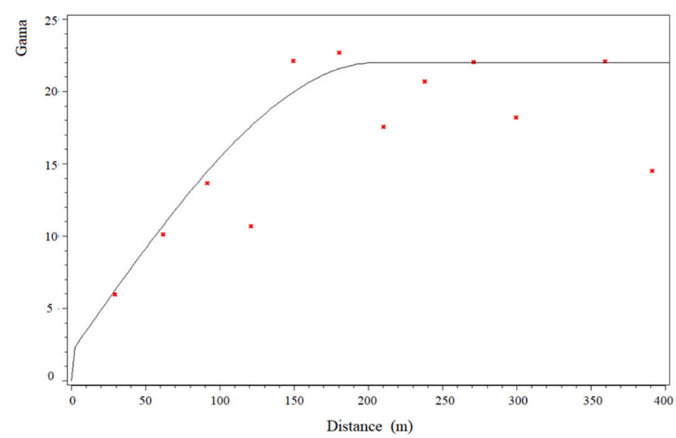

Fig. 3. Experimental omnidirectional variogram and the fitted model to it.

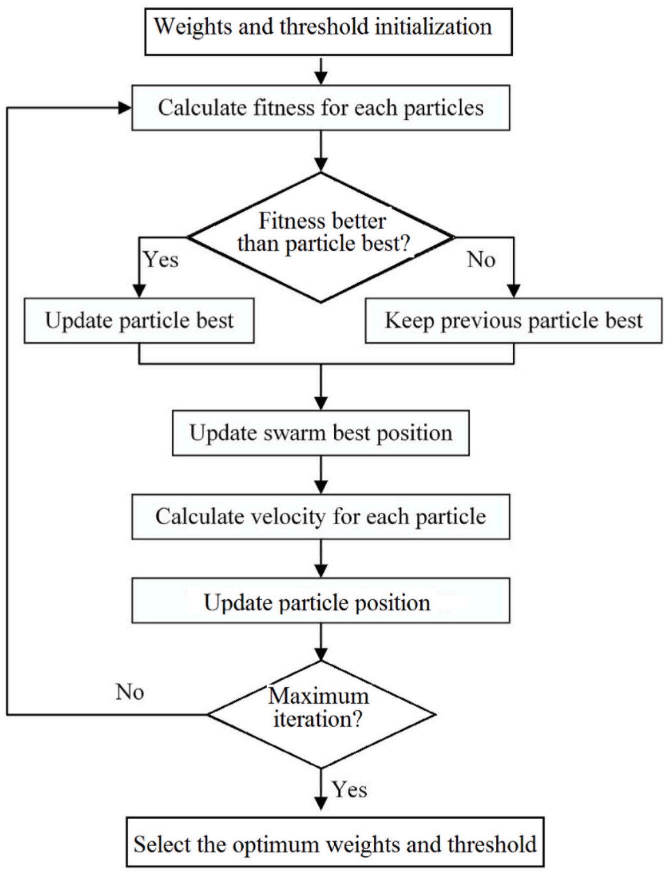

Fig. 4. The PSO algorithm flowchart.

bauxite, Clayey soft bauxite, and Kaolinitic clay, from top to bottom, can be seen in the survey of drill holes, respectively. Since only hard bauxite has played a critical role in the alumina production, this lithological domain is known as ore deposit. In this paper, the Aluminum oxide (Al_2O_3) grade has been estimated in the hard bauxite domain based on 362 samples taken from drill cores. Fig. 2 shows the histogram of Al_2O_3 grade. Moreover, Table 1 reports the descriptive statistics of Al_2O_3 grade using these samples. Spatial variability has been investigated by fitting a spherical model to an experimental omnidirectional variogram of Al_2O_3 grade within the domain (Fig. 3). Due to relatively limited number of samples, investigation of grade anisotropy is impossible in this study.

The 3D geological model of the study area has been developed using geoscience datasets, including a geological map, geological cross-sections, a topography map and drill core samples. Then 3D block model has been constructed by filling the geological model with 5m × 5m × 5m blocks and 2.5 m × 2.5m × 2.5m subblocks. The block model consists of 168,564 blocks.

3. Material and methods

The PSO was introduced in 1995 by Eberhart and Kennedy (Kennedy and Eberhart 1995). It is a robust technique to find an overall optimum solution in a multidimensional search space (Esfe et al., 2018; Parsopoulos and Vrahatis 2002; Hajihassani et al., 2018). PSO has several advantages over other optimization algorithms, including appropriate performance on optimization of a nonlinear function, simplicity and easy implementation, and fast convergent (Chen et al., 2011). This algorithm has been appropriately used to optimize problems induced by social behaviors, such as bird swarm (Trelea 2003). Clustering of individuals is performed in the PSO algorithm for efficiently solving optimization problems. First, each individual is considered as one particle. Then, the velocity of each particle is adjusted relatively to the best position found by the particle and the best position found by the neighborhood. More precisely, the PSO process is performed in the following stages: swarm initialization, updating swarm best position, calculating velocity for each particle, updating the position of particles, estimating with fitness function, and finalizing by a stop decision. Fig. 4 demonstrates the algorithm flowchart of the PSO.

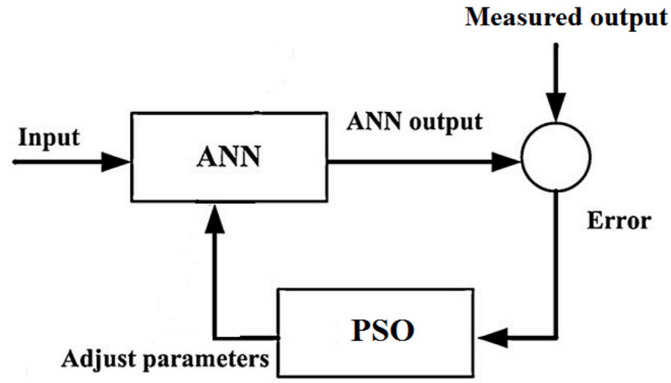

Fig. 5. Schematic diagram of BPANN-PSO.

This paper proposes a hybrid method (i.e., BPANN-PSO) to solve the grade estimation problem, which exploits the PSO algorithm for optimization of the network architecture. Fig. 5 shows the applied BPANN-PSO method. The initial weight and threshold of the artificial neural network are selected as a swarm of particles for starting the PSO process. The particle collection makes a swarm. The fitness of particles' position is validated using the mean square error (MSE) on the training set. The artificial neural network architecture that gets a higher fitness value will be considered as the best position of the swarm. The next swarm is produced by considering the position-update of particles according to both the best position of the swarm and each particle in history. The particle swarm gradually moves to the optimum position of the solution until reaching the maximum number of iterations. During the PSO process, the position update of particles is performed as following (Qi et al., 2018):

$$V_i^{t+1} = wV_i^t + c_1 r_1 \left(p_{best,i}^t - X_i^t\right) + c_2 r_2 \left(g_{best,\ i}^t - X_i^t\right) \tag{1}$$

$$X_i^{t+1} = X_i^t + V_i^{t+1} \tag{2}$$

where, V_i^{t+1} and V_i^t are the velocity of particle i at iterations t and $t+1$, respectively, X_i^{t+1} and X_i^t are the position of particle i at iterations t and $t+1$, respectively; w is the inertia parameter; c_1 is the cognitive influence parameter; c_2 is the social influence parameter; $p_{best,i}^t$ is the best position of a particle; $g_{best,i}^t$ is the swarm's best position; and r_1 and r_2 are random values between 0 and 1.

The best solution by the PSO algorithm is considered as the initial weights and threshold of the BPANN. Afterward, the BPANN is applied for network training.

4. Grade modeling using BPANN-PSO

To predict the Al_2O_3 grade, BPANN and BPANN-PSO are applied. The dataset consisting of 362 samples is split into two subsets (i.e., train and test). A subset of 295 samples - about 80% of the total-is used for training and the rest of the samples are used for models' testing. For building a model with good generalization performance, the data set should be carefully split between the training and testing datasets. It is important to make these sets with 1) the same statistical characteristics, and 2) enough spatial distance. The presence of a high spatial correlation between the samples in train and test subsets will lead to over-optimistic estimation. To deal with this issue, the trained model should be

Table 2
Statistical parameters of train and test datasets.

	Train	Test
Number of Samples	295	67
Mean	42.44	42.93
Min	25	35.38
Max	63.15	52.2
Var	24.29	14.46
Median	42.25	43.49
Lower Quartile	39.1	40.19
Upper Quartile	45	45.5

evaluated based on a test dataset that its samples are not close to the samples of the train dataset (Roberts et al., 2017; Pohjankukka et al., 2017; Hoffimann et al., 2021). To this end, 14 drillholes (about 20% of drillholes) were selected based on a trial-and-error procedure, in such a way that 1) one drillhole was selected from each part of the region, 2) Al_2O_3 grade in the samples taken from these drillholes has a statistical distribution similar to the rest of samples. Statistical parameters of train and test datasets are summarized in Table 2. Despite differences in some statistical parameters (such as min, max and variances), this combination was the best covering all parts of area.

The network architecture, as shown in Fig. 6(a), is a BPANN with input, hidden and output layers. The network receives ten inputs: the coordinates of estimation point (the first three nodes in the input layer are the easting, northing and elevation of estimation point (red cycle in Fig. 6(b))), the distance between the estimation point and the surrounding samples (nodes 4, 6, 8, and 10 of input layer), and the grade of the surrounding samples (nodes 5,7,9 and 10 in the input layer). The surrounding samples have been selected based on the quadrant search algorithm to ensure that one drill hole (or one cluster of samples) does not overwhelm the grade estimate and thus induces bias. At the margins of the study area, the quadrant search does not find any sample in any of the quadrants, thus will generate some missing values. To solve this problem, a dynamic search strategy has been used and missing values have been replaced by choosing more samples from the filled quadrant. The network has two hidden layers. The first and second hidden layer nodes are set to 30 and 27 nodes, respectively. The optimum numbers of nodes in hidden layers are determined based on the trial-and-error method. The output layer has one node providing the estimated grade.

The size of the swarm and the maximum number of iterations were determined to be 300 and 1000 by trial and error during modeling. The w, c_1 and c_2 were selected to be 0.73, 1.5, and 1.5 based on the proposed method by Clerc and Kennedy (Clerc and Kennedy 2002; Qi et al., 2018). The convergence rate of the algorithm is illustrated in Fig. 7.

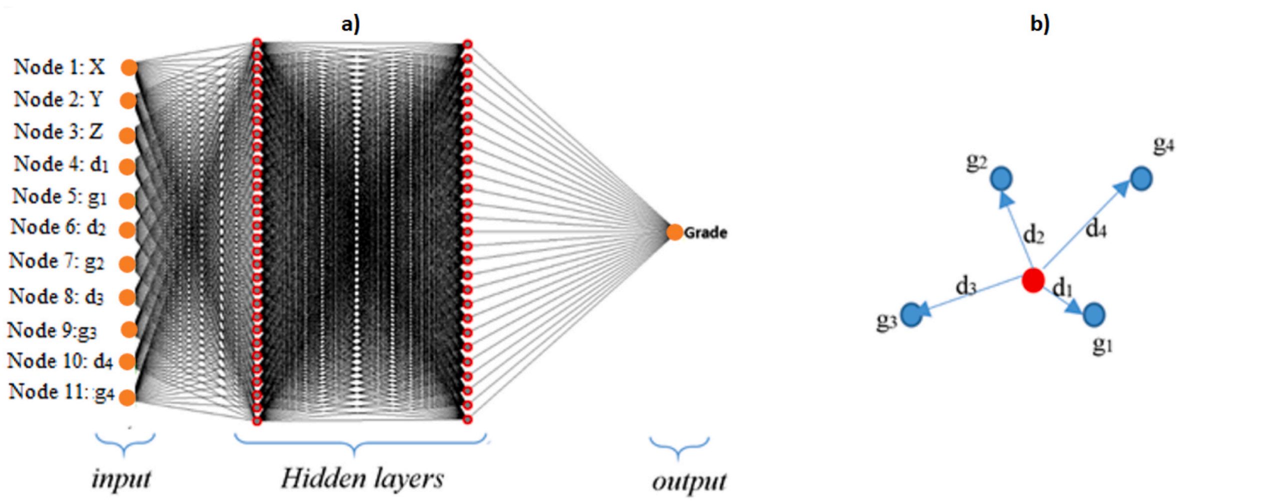

Fig. 6. The configuration of input data for modeling. a) The BPANN architecture for grade modelling, and b) Estimation point (red circle) and selected neighbor samples (blue circles) using the octant search algorithm. (For interpretation of the references to colour in this figure legend, the reader is referred to the Web version of this article.)

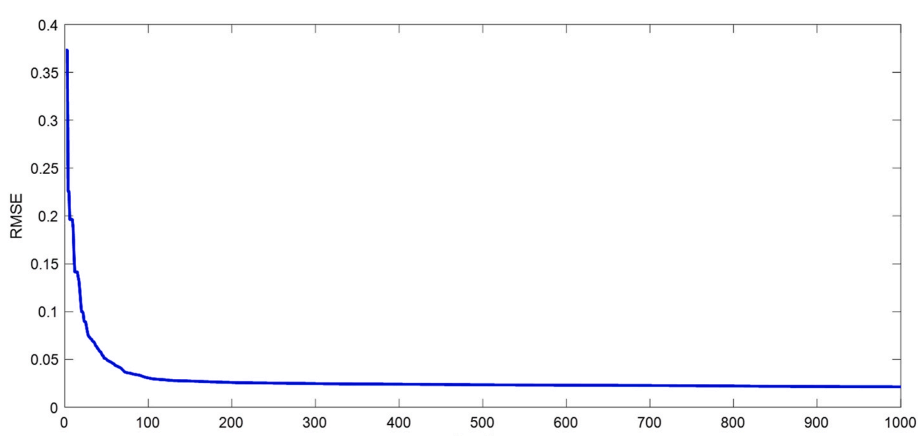

Fig. 7. The optimization process for the objective function in PSO algorithm.

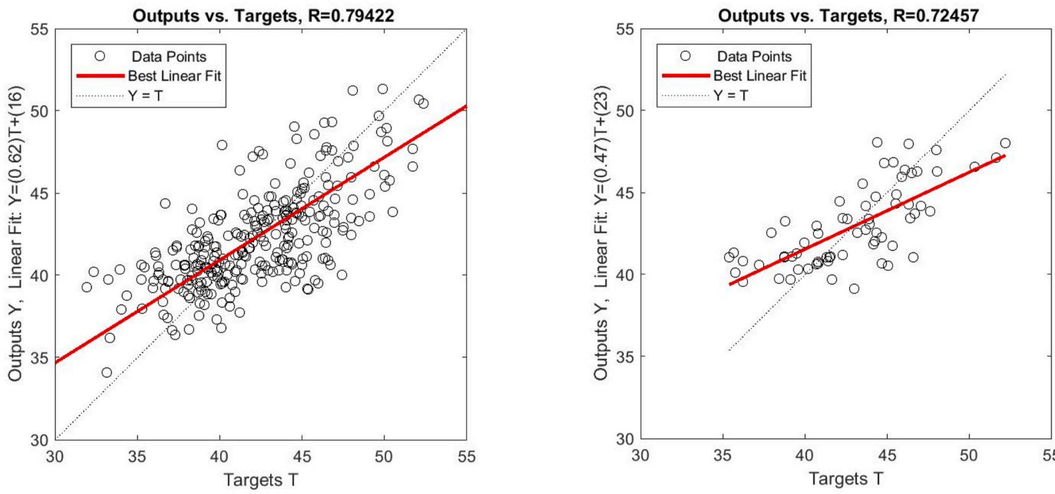

Fig. 8. The BPANN-PSO model performance to predict the Al_2O_3 grade in train (left) and test (right) datasets.

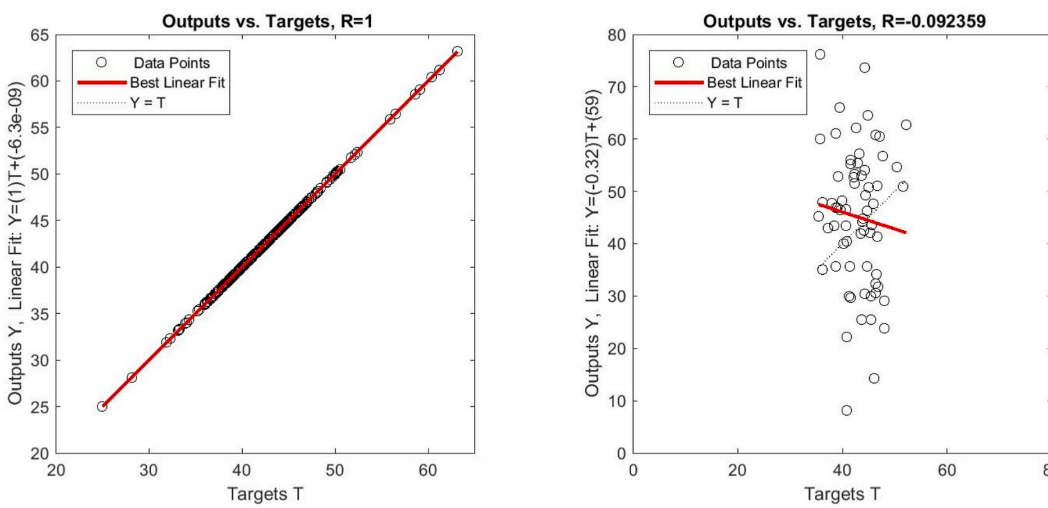

Fig. 9. The BPANN model performance to predict the Al_2O_3 grade in train (left) and test (right) datasets.

Table 3
The values of statistical functions for the models.

Model	Statistical functions			
	R		MSE	
	Train	Test	Train	Test
BPANN-PSO	0.79	0.72	8.93	6.85
BPANN	1	−0.09	1.3E-15	203
Ordinary Kriging	–	0.32	–	13.60

5. Results and discussion

The accuracy of the BPANN-PSO model was evaluated using multiple statistical functions such as correlation coefficient (R) and mean squared error (MSE). The correlation coefficient between measured and estimated grades using the BPANN-PSO model are 0.79 and 0.72 in training and testing, respectively (Fig. 8). As can be seen in Fig. 9, the correlation coefficients between measured and predicted grades for the training and testing by the BPANN model are 1 and -0.09, respectively, which shows the overfitting problem in the results. The correlation coefficients and the MSE of the BPANN-PSO and BPANN models are summarized in Table 3. The R and MSE of testing for the BPANN-PSO model is better

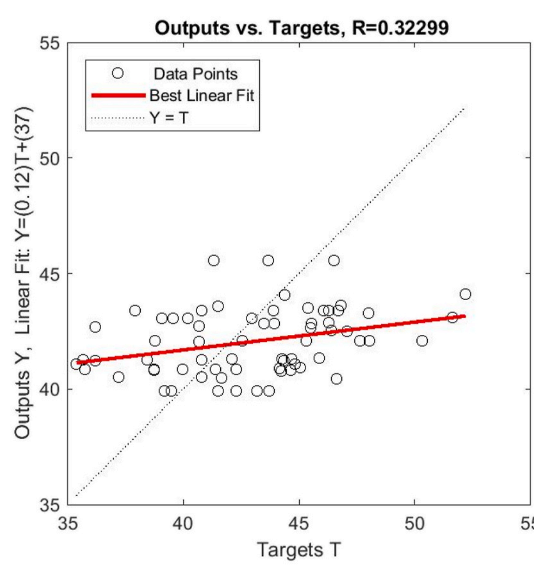

Fig. 10. Comparison of real and predicted Al_2O_3 grade based on the ordinary kriging in test dataset.

Table 4
Results of the defined scenarios for number of Surrounding samples in input space configuration.

Number of Surrounding samples in input space configuration	Number of Dimensions	Dimensions	Correlation coefficient		MSE	
			Train	Test	Train	Test
0	3	X-Y-Z	0.55	0.41	16.9	15.9
1	5	X-Y-Z of estimation point + Grades and distances of nearest sample	0.54	0.48	16.2	15.2
2	7	X-Y-Z of estimation point + Grades and distances of 2 nearest samples	0.70	0.51	11.73	15.87
3	9	X-Y-Z of estimation point + Grades and distances of 3 nearest samples	0.64	0.33	12.5	26.3
4	11	X-Y-Z of estimation point + Grades and distances of 4 nearest samples	0.79	0.72	8.9	6.8
5	13	X-Y-Z of estimation point + Grades and distances of 5 nearest samples	0.70	0.27	11.9	101.1
6	15	X-Y-Z of estimation point + Grades and distances of 6 nearest samples	0.59	0.25	16.2	37.0
7	17	X-Y-Z of estimation point + Grades and distances of 7 nearest samples	0.71	0.12	12.2	18.8
8	19	X-Y-Z of estimation point + Grades and distances of 8 nearest samples	0.65	0.27	13.4	20.0

than these values of the BPANN model, indicating the higher performance of the BPANN-PSO model than BPANN for the Al_2O_3 grade prediction. Although the accuracy of BPANN is higher than BPANN-PSO in training, the BPANN-PSO outperforms the BPANN algorithm in testing. This indicates the low generalization of the BPANN algorithm.

In the mining industry, the ordinary Kriging method is known as the most popular grade estimation method. Therefore, the performance of the ordinary kriging method has been investigated to be compared to the performance of BPANN-PSO. The same training and test data split are used to compare the kriging algorithm to BPANN-PSO and BPANN. The variable has been estimated at test samples based on the training dataset and the performance parameters of R and MSE have been calculated. The results have been summarized in Table 3. The correlation coefficient between measured and estimated grades for ordinary kriging method is 0.32 in testing (Fig. 10). Table 3 indicates that BPANN-PSO has better performance than ordinary kriging method in this case study.

One of the most common problems with spatial estimators is smoothing bias. Smoothing bias can be defined as underestimation of high values and overestimation of low values. With smoothing bias, the variance of the estimated values is smaller than the variance of the data and smaller than the variance of the true values at the estimation locations (Bourgault, 2021). Figs. 8–10 show that the BPANN-PSO, BPANN and ordinary kriging estimators are affected by smoothing bias. However, BPANN-PSO performs much better in terms of smoothing bias compared to ordinary kriging and BPANN.

The number of surrounding samples is one of the most important parameters in defining the input space configuration. To investigate the sensitivity of the results to the number of surrounding samples, an experiment has been designed. In this experiment, nine various configurations have been defined by varying this parameter between 0 and 8 (Table 4). Table 4 summarizes the results of training and validating these data configurations by PSO-BPANN. It can be concluded that a slight change in the number of surrounding samples will lead to changes in the performance of the model. In this experiment, the optimum number of surrounding samples is four. This number can be interpreted as the result of low grade variability, low thickness of bauxite layer, number of available data, and pattern of exploratory drilling. It should be mentioned that the optimum number of surrounding samples is case dependent and its optimum value should be tunned.

To evaluate the effect of using proposed configuration (X-Y-Z coordinates + neighbor samples configuration and variability), a comparison has been made with the ordinary configurations based on the correlation coefficient and mean square error (MSE) of trained BPANN-PSO. Table 5 summarizes the results of using different data configurations. Several conclusions can be obtained from the results reported in Table 5. First and foremost, it is noticeable that the proposed data configuration, which includes both the global trend (by putting coordinate of estimation point in the input layer) and local variability around estimation point, outperforms using other configurations. The first input space configuration takes into account grade as a function of coordinate and defines the projection from the input coordinate space to the grade vector during training. The second one, however, only considers the relation between surrounding samples (their grades and distances to estimation point) and the grade of estimation point.

Finally, the Al_2O_3 grade has been estimated in the geological block model using the trained BPANN-PSO model. For this purpose, coordinates of the center of each block have been considered as the coordinates of the estimation point (nodes 1,2, and 3 of the input layer in Fig. 6). A simple MATLAB script has been developed to find the distances between the center of each block and the surrounding samples (nodes 4, 6, 8, and 10 of the input layer in Fig. 6), and the grade of the surrounding samples (nodes 5,7,9 and 10 of the input layer in Fig. 6). The estimated block model is shown in Fig. 11.

6. Conclusions

This study proposes to integrate BPANN and PSO algorithms for the purpose of grade estimation. In the proposed BPANN-PSO model, the PSO algorithm is applied to optimize the weights and the threshold of BPANN. This integration overcomes the local minima problem of the BPANN algorithm. Moreover, this paper proposes a new neural network input space configuration to address the generalization problem of the BPANN algorithm in the grade estimation task. It includes spatial variability by exploiting the coordinates of the estimation point, the distance between the estimation point and the surrounding samples, and the

Table 5
Results of the defined scenarios for input space configuration.

Input space configuration	Number of Dimensions	Dimensions	Correlation coefficient		MSE	
			Train	Test	Train	Test
Sample coordinates	3	X-Y-Z	0.55	0.41	16.86	15.97
Surrounding samples	8	Grades and distances of 4 nearest samples	0.81	−0.22	8.19	42.59
Sample coordinates and Surrounding samples	11	X-Y-Z of estimation point + Grades and distances of 4 nearest samples	0.79	0.72	8.93	6.85

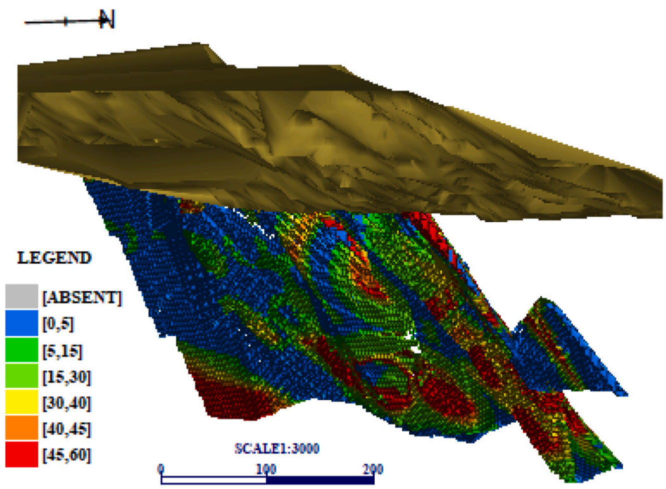

Fig. 11. Estimated block model in Zu2 Jajarm deposit (view direction: Azi 290, dip 5).

grade of the surrounding samples as input. The proposed BPANN-PSO estimation technique was applied for the Al_2O_3 grade estimation in a dataset acquired from the largest bauxite deposit in Iran. The testing set R values of the Al_2O_3 grade estimation using BPANN-PSO, BPANN and ordinary kriging were 0.72, −0.09, and 0.32, respectively. Additionally, the testing set MSE values of the Al_2O_3 grade estimation using these methods were 6.85, 203 and 13,6, respectively The R and MSE values of the testing sets in the BPANN-PSO model are less than those in the BPANN and ordinary kriging models. This indicates the higher efficiency of BPANN-PSO for grade estimation. This study has demonstrated that the proposed model could be applied to estimate the grade in the mineral resource evaluation with a reasonable error.

Moreover, we performed a comprehensive analysis of the proposed input space configuration that considers both the coordinate of the estimation point and the surrounding samples. Comparing the models trained based on the proposed configuration and the previous ones (based on the performance parameters of R and MSE) shows that the proposed data configuration outperforms using other configurations.

Considering the local variability in the input space configuration would be effective on the reproduction of spatial statistics. But in this research, due to the limited number of samples in the test dataset, assessing the reproduction of spatial statistics was impossible. It is suggested that in future research this issue be evaluated by selecting a case study with a larger number of samples.

In this manuscript, the workflow is defined based on the quadrant search algorithm and the number of surrounding samples is considered 4. Any change in this parameter could change the performance of the method. Optimization of the number of surrounding samples remains as future research.

Availability of data and materials

The datasets used and analyzed during the current study are available from the corresponding author on reasonable request.

Author contributions

Saeed Soltani-Mohammadi: Methodology, data preprocessing, validation, writing, supervision. **Fatemeh Sadat Hoseinian:** Methodology, software, validation, formal analysis, visualization, writing. **Maliheh Abbaszadeh:** Methodology, validation, formal analysis, visualization, interpretation, writing. **Mahdi Khodadadzadeh:** validation, writing.

Computer code availability

The code "PBANN-PSO" was developed in MATLAB. The code is available for download from the following public repository: https://github.com/saeedsoltan/cageo.

Declaration of competing interest

The authors declare that they have no known competing financial interests or personal relationships that could have appeared to influence the work reported in this paper.

Acknowledgements

The authors are indebted to Dr Ute Mueller and the anonymous reviewers for their valuable and constructive comments on an earlier draft of this paper. The studies reported in this manuscript were supported by a grant from the University of Kashan (Grant No. 986017).

References

Abbaszadeh, M., Hezarkhani, A., Soltani Mohammadi, S., 2016. Proposing drilling locations based on the 3D modeling results of fluid inclusion data using the support vector regression method. J. Geochem. Explor. 165, 23–34.
Badel, Mehdi, Angorani, Saeed, Shariat Panahi, Masoud, 2011. The application of median indicator kriging and neural network in modeling mixed population in an iron ore deposit. Comput. Geosci. 37, 530–540.
Bourgault, G., 2021. Clarifications and new insights on conditional bias. Math. Geosci. 53, 623–654. https://doi.org/10.1007/s11004-020-09853-6.
Changwei, Yang, Li, Zonghao, Guo, Xueyan, Yu, Wenying, Jin, Jing, Zhu, Liang, 2019. Application of BP neural network model in risk evaluation of railway construction. Complexity 2946158, 2019.
Chatterjee, Snehamoy, Bhattacherjee, Ashis, Samanta, Biswajit, Pal, Samir, 2006. Ore grade estimation of a limestone deposit in India using an Artificial Neural Network. Appl. GIS 2.
Chen, Debao, Zhao, Chunxia, Zhang, Haofeng, 2011. An improved cooperative particle swarm optimization and its application. Neural Comput. Appl. 20, 171–182.
Clerc, Maurice, Kennedy, James, 2002. The particle swarm-explosion, stability, and convergence in a multidimensional complex space. Evolutionary Computation, IEEE Transactions on 6, 58–73.
Dutta, S., Bandopadhyay, S., Ganguli, R., Misra, D., 2010. 'Machine learning algorithms and their application to ore reserve estimation of sparse and imprecise data. J. Intell. Learn Syst. Appl. 2, 86–96.
Esfe, Hemmat, Mohammad, Mahian, Omid, Hadi Hajmohammad, Mohammad, Wongwises, Somchai, 2018. 'Design of a heat exchanger working with organic nanofluids using multi-objective particle swarm optimization algorithm and response surface method. Int. J. Heat Mass Tran. 119, 922–930.
Esmaeily, Dariush, Rahimpour-Bonab, Hossain, Esna-Ashari, Amir, Ali, Kananian, 2010. Petrography and geochemistry of the Jajarm Karst bauxite ore deposit, NE Iran: implications for source rock material and ore genesis. Turk. J. Earth Sci. 1.

Guo, William, 2010. `A novel application of neural networks for instant iron-ore grade estimation. Expert Syst. Appl. 37, 8729–8735.

Hajihassani, M., Armaghani, D Jahed, Kalatehjari, R., 2018. 'Applications of particle swarm optimization in geotechnical engineering: a comprehensive review. Geotech. Geol. Eng. 36, 705–722.

Hoffimann, J., Zortea, M., de Carvalho, B., Zadrozny, B., 2021. Geostatistical Learning: Challenges and Opportunities. arXiv Prepr arXiv210208791.

Hoseinian, Sadat, Fatemeh, Abdollahzade, Aliakbar, Mohamadi, Saeed Soltani, Hashemzadeh, Mohsen, 2017. Recovery prediction of copper oxide ore column leaching by hybrid neural genetic algorithm. Trans. Nonferrous Metals Soc. China 27, 686–693.

Hoseinian, Sadat, Fatemeh, Abdollahzadeh, Aliakbar, Rezai, Bahram, 2018. Semi-autogenous mill power prediction by a hybrid neural genetic algorithm. J. Cent. S. Univ. 25, 151–158.

Hoseinian, Sadat, Fatemeh, Rezai, Bahram, Kowsari, Elaheh, Safari, Mehdi, 2019. A hybrid neural network/genetic algorithm to predict Zn (II) removal by ion flotation. Separ. Sci. Technol. 1–10.

Jafrasteh, Bahram, Fathianpour, Nader, 2017. A hybrid simultaneous perturbation artificial bee colony and back-propagation algorithm for training a local linear radial basis neural network on ore grade estimation. Neurocomputing 235, 217–227.

Jafrasteh, B., Fathianpour, N., Suárez, A., 2016. Advanced Machine Learning Methods for Copper Ore Grade Estimation. European Association of Geoscientists & Engineers, pp. 495–400087.

Jafrasteh, Bahram, Fathianpour, Nader, Alberto, Suárez, 2018. `Comparison of machine learning methods for copper ore grade estimation. Comput. Geosci. 22, 1371–1388.

Kapageridis, Ioannis, 2005. `Input space configuration effects in neural network-based grade estimation. Comput. Geosci. 31, 704–717.

Kapageridis, Ioannis, Bryan, Denby, 1998. Neural network modelling of ore grade spatial variability. In: International Conference on Artificial Neural Networks. Springer, Bratislava, Slovakia, pp. 209–214.

Kapageridis, Ioannis, Denby, B., 1999. Ore Grade Estimation with Modular Neural Network Systems - A Case Study.

Kaplan, Umit, Topal, Erkan, 2020. A new ore grade estimation using combine machine learning algorithms. Minerals 10, 847.

Kennedy, J., Eberhart, R., 1995. Particle swarm optimization. In: Proceedings of ICNN'95 - International Conference on Neural Networks, 4, pp. 1942–1948.

Li, Xiao-li, Xie, Yu-ling, Guo, Qian-jin, Li, Li-hong, 2010. Adaptive ore grade estimation method for the mineral deposit evaluation. Math. Comput. Model. 52, 1947–1956.

Mahmoudabadi, Hamid, Izadi, Mohammad, Menhaj, Mohammad Bagher, 2009. A hybrid method for grade estimation using genetic algorithm and neural networks. Comput. Geosci. 13, 91–101.

Matias, Jose, Vaamonde, Antonio, Taboada, J., Gonzãlez-Manteiga, Wenceslao, 2004. Support vector machines and gradient boosting for graphical estimation of a slate deposit. Stoch. Environ. Res. Risk Assess. 18, 309–323.

Parsopoulos, Konstantinos E., Vrahatis, Michael N., 2002. Recent approaches to global optimization problems through particle swarm optimization. Nat. Comput. 1, 235–306.

Pohjankukka, J., Pahikkala, T., Nevalainen, P., Heikkonen, J., 2017. Estimating the prediction performance of spatial models via spatial k-fold cross validation. Int. J. Geogr. Inf. Sci. 31, 2001–2019. https://doi.org/10.1080/13658816.2017.1346255.

Qi, Chongchong, Fourie, Andy, Chen, Qiusong, 2018. Neural network and particle swarm optimization for predicting the unconfined compressive strength of cemented paste backfill. Construct. Build. Mater. 159, 473–478.

Rendu, J.-M., 2014. An Introduction to Cut-Off Grade Estimation. Society for Mining, Metallurgy, and Exploration.

Roberts, D.R., Bahn, V., Ciuti, S., et al., 2017. Cross-validation strategies for data with temporal, spatial, hierarchical, or phylogenetic structure. Ecography 40, 913–929. https://doi.org/10.1111/ecog.02881.

Samanta, Biswajit, 2002. `Data segmentation and genetic algorithms for sparse data division in nome placer gold grade estimation using neural network and geostatistics. Explor. Min. Geol. 11, 69–76.

Samanta, B., Bandopadhyay, S., 2009. Construction of a radial basis function network using an evolutionary algorithm for grade estimation in a placer gold deposit. Comput. Geosci. 35, 1592–1602.

Samanta, Biswajit, Ganguli, Rajive, Bandopadhyay, Sukumar, 2005. Comparing the predictive performance of neural networks with ordinary kriging in a bauxite deposit. Min. Technol. 114, 129–139.

Samanta, Biswajit, Bandopadhyay, Sukumar, Ganguli, Rajive, 2006. `Comparative evaluation of neural network learning algorithms for ore grade estimation. Math. Geosci. 38, 175–197.

Sinclair, A., Blackwell, G., 2002. Applied mineral inventory estimation. In: Appl Miner Invent Estim by Alastair J Sinclair Garst H Blackwell. UK Cambridge Univ Press, Cambridge, p. 400. https://doi.org/10.1017/CBO9780511545993, 0521791030, May 2002.

Singh, R.K., Ray, D., Sarkar, B.C., 2018. Recurrent neural network approach to mineral deposit modelling. In: 2018 4th International Conference on Recent Advances in Information Technology. RAIT), pp. 1–5.

Tahmasebi, Pejman, Hezarkhani, Ardeshir, 2012. `A hybrid neural networks-fuzzy logic-genetic algorithm for grade estimation. Comput. Geosci. 42, 18–27.

Tahmasebi, Pejman, Hezarkhani, Ardeshir, 2010. Application of adaptive neuro-fuzzy inference system for grade estimation; case study, sarcheshmeh porphyry copper deposit, kerman, Iran. Australian Journal of Basic and Applied Sciences 4, 408–420.

Tenorio, Victor Octavio, Bandopadhyay, Sukumar, Misra, Debasmita, Naidu, Sathy, Kelley, John, 2015. Support vector machines applied for resource estimation of underwater glacier-type platinum deposits. In: *Application Of Computers and Operations Research in the Mineral Industry*, 889-902. Society for Mining, Metallurgy, and Exploration, United States.

Trelea, Ioan Cristian, 2003. The particle swarm optimization algorithm: convergence analysis and paramAustralian Journal of Basic and Applied Scienceseter selection. Inf. Process. Lett. 85, 317–325.

Wu, Xiping, Zhou, Yingxin, 1993. 'Reserve estimation using neural network techniques. Comput. Geosci. 19, 567–575.

Yamamoto, J.K., 1999. Quantification of uncertainty in ore-reserve estimation: applications to Chapada copper deposit, State of Goiás, Brazil. Nat. Resour. Res. 8, 153–163.